Hybrid meson decay phenomenology

Philip R. Page
Theoretical Division, Los Alamos National Laboratory, Los Alamos, New Mexico 87545

Eric S. Swanson
Department of Physics, North Carolina State University, Raleigh, North Carolina 27695-8202
and Jefferson Laboratory, 12000 Jefferson Avenue, Newport News, Virginia 23606

Adam P. Szczepaniak
Department of Physics, Indiana University, Bloomington, Indiana 47405-4202
(Received 19 August 1998; published 8 January 1999)

The phenomenology of a newly formulated model of hybrid meson decay is developed. The decay mechanism is based on the heavy quark expansion of QCD and the strong coupling flux tube picture of nonperturbative glue. A comprehensive list of partial decay widths of a wide variety of light, $s\bar{s}$, $c\bar{c}$, and $b\bar{b}$ hybrid mesons is presented. Results which appear approximately universal are highlighted along with those which distinguish different hybrid decay models. Finally, we examine several interesting hybrid candidates in detail. [S0556-2821(99)01105-4]

PACS number(s): 12.39.Mk, 13.25.Jx

I. INTRODUCTION

Quantum chromodynamics at low energy remains enigmatic chiefly because of an almost complete lack of knowledge of the properties of soft glue. Glue must certainly be understood if phenomena such as color confinement, mass generation, and dynamical symmetry breaking are to be understood. The discovery and explication of hadrons with excited gluonic degrees of freedom is clearly an important step in this process. Furthermore, the search for nonperturbative glue, in particular as manifested in hybrid mesons, would be greatly facilitated by a rudimentary knowledge of the hybrid spectrum and decay characteristics. Although it appears that lattice estimates of light quenched hybrid masses are forthcoming [1], hadronic decays remain difficult to calculate on the lattice. Thus one is forced to rely on model estimates of the couplings of hybrids to ordinary mesons.

Historically, there have been two approaches to such estimates. The first assumes that hybrids are predominantly quark-antiquark states with an additional constituent gluon [2] and that decays proceed via constituent gluon dissociation [3]. The second assumes that hybrids are quark-antiquark states moving on an adiabatic surface generated by an excited ''flux tube'' configuration of glue [4]. Decays then proceed by a phenomenological pair production mechanism (the ''$^3P_0$ model'') coupled with a flux tube overlap [5]. An important feature of this model is that the quark pair creation vertex is uncorrelated with the gluonic modes of the hybrid.

A third possibility for hybrid decay has been recently introduced [6]. This model also assumes flux tube hybrids but employs a different decay vertex. The vertex is constructed by using the heavy quark expansion of the Coulomb gauge QCD Hamiltonian to identify relevant operators. The gluonic portion of these are then evaluated using a slightly extended version of the flux tube model of Isgur and Paton [4]. The essential new feature is that the gluon field operator is expressed in terms of the nonperturbative phonon modes of the flux tube model rather than traditional plane waves.

This paper begins with a review of the development of the decay model of Ref. [6] and describes in detail several issues which arise in converting the amplitudes to decay widths. We then summarize the main general features of the model and compare these with the flux tube decay model of Isgur, Kokoski, and Paton (IKP). The main portion of this work is a comprehensive review of the decay modes of all low lying isovector, isoscalar, $s\bar{s}$, $c\bar{c}$, and $b\bar{b}$ $2^{\mp\pm}$, $1^{\pm\pm}$, $1^{\mp\pm}$, and $0^{\mp\pm}$ hybrids. A detailed discussion of interesting features in the phenomenology of these states follows.

II. HYBRID DECAY AMPLITUDE

The first step in the construction of any hybrid decay model is determining what is meant by a hybrid. We stress that choosing a model of hybrids with the correct degrees of freedom is crucial because decays probe the internal structure of the participating particles. Thus for example, in the flux tube model low lying vector hybrids must have the quarks in a spin singlet and this implies that vector hybrids may not decay to a pair of spin zero mesons (see below for further discussion of this point). However, this need not be true in a model which assigns hybrid quantum numbers differently (for example, it is possible to construct spin one vector hybrids in constituent glue models). In this work, we choose to employ a slightly modified version of the flux tube model hybrids of Isgur and Paton, as described in Refs. [6, 7]. Recent lattice calculations of adiabatic hybrid potential surfaces show that the flux tube model does a good job of describing the level orderings and degeneracies apparent in the data (although it does not reproduce many details) [8]. Thus one may be confident that the model captures the essential features of (heavy) hybrid structure necessary for the construction of a viable decay model.

The flux tube model of Isgur and Paton [4] is extracted

from the strong coupling limit of the QCD lattice Hamiltonian. The Hamiltonian is first split into blocks of distinct ''topologies'' (in reference to possible gauge invariant flux tube configurations) and then adiabatic and small oscillation approximations of the flux tube dynamics are made to arrive at an N-body discrete string-like model Hamiltonian for gluonic degrees of freedom. This is meant to be operative at intermediate scales $a \sim b^{-1/2}$ where the strong coupling is of order unity. The lattice spacing is denoted by a, the string tension by b, and there are N ''beads'' (or links) evenly spaced between the $Q\overline{Q}$ pair. Diagonalizing the flux tube Hamiltonian yields phonons, $\alpha^a_{m,\Lambda}$, which are labelled by their color (a), mode number (m), and polarization (Λ). A hybrid may be built of $n_{m\Lambda}$ phonons in the m'th mode with polarization $\Lambda = \pm$. In particular, hybrid states with a single phonon excitation are constructed as

$$|H\rangle \sim \int d\mathbf{r}\, \varphi_H(r)\, \chi^{PC}_{\Lambda,\Lambda'} D^{L_H^*}_{M_L,\Lambda}(\phi,\theta,-\phi) \times T^a_{ij}\, b^\dagger_i(\mathbf{r}/2) d^\dagger_j(-\mathbf{r}/2) \alpha^{a\dagger}_{m,\Lambda'} |0\rangle. \quad (1)$$

Spin and flavor indices have been suppressed and color indices are explicit [the matrices T^a are the generators of SU(N_c)]. The factor $\chi^{PC}_{\Lambda,\Lambda'}$ in the hybrid wave function projects onto states of good parity and charge conjugation. The quantum numbers of these states are given by $P = \eta_{PC}(-)^{L_H+1}$ and $C = \eta_{PC}(-)^{L_H+S_H+N}$ where $\eta_{PC} = \chi^{PC}_{-1,-1} = \pm 1$ and $N = \Sigma_m m(n_{m+} + n_{m-})$. These expressions differ from Isgur and Paton [4] because we have adopted the standard definitions for the polarization vectors and the Wigner rotation matrix, following the Jacob-Wick conventions. We shall consider low-lying hybrids only so that $m = 1$ in what follows.

It remains to specify the structure of the decay operator. To leading order in the hopping parameter and strong coupling expansion, one can show that the operator for producing a $q(\mathbf{r}_q)\overline{q}(\mathbf{r}_{\overline{q}})$ pair has the following structure [9]:

$$F_{q\overline{q}} \propto e^{-m|\mathbf{r}_{q\overline{q}}|} b^\dagger(\mathbf{r}_q) \mathbf{r}_{q\overline{q}} \cdot \boldsymbol{\sigma} d^\dagger(\mathbf{r}_{\overline{q}}). \quad (2)$$

The dependence on the relative distance, $\mathbf{r}_{q\overline{q}} = \mathbf{r}_q - \mathbf{r}_{\overline{q}}$, comes from integrating $n = |\mathbf{r}_{q\overline{q}}|/a$ products of link operators from the kinetic term

$$K = -\kappa m \sum_{n,\mu} \overline{\psi}_n (1+\gamma^\mu) U_{n,\mu} \psi_{n+\mu} + \text{H.c.}, \quad (3)$$

over a straight line in the direction of $\mathbf{r}_{q\overline{q}}$. Here, κ is the Wilson hopping parameter and $U_{n,\mu}$ is a link operator at site n and direction μ. The prefactor $e^{-m|\mathbf{r}_{q\overline{q}}|} = (2\kappa)^n$ can be identified with the Schwinger tunneling factor for pair production in an external field of the parent $q\overline{q}$ meson. In our picture, hybrids are characterized by excitations of the gluonic field. We will therefore assume that hybrid decays can proceed through local de-excitation of this field rather then by quark tunneling in the external field of the meson source. Thus the expectation value of the gluon operator in K between excited (hybrid) and de-excited (low lying meson decay products) is used to obtain the effective $q\overline{q}$ production operator. In [6] the chromoelectric **E** and **B** fields have been mapped onto the flux tube space of gluon excitations described by the phonon operators. Using these expressions together with $\mathbf{E} = -d\mathbf{A}/dt$ one then obtains

$$A^a_\lambda(\mathbf{x}_n, t) = \frac{-i}{a\sqrt{(N+1)}} \sum_m \cos\left(\frac{m\pi}{N+1} n\right) \frac{1}{\sqrt{a\omega_m}} (\alpha^a_{m\lambda} e^{-i\omega_m t} - \alpha^{a\dagger}_{m\lambda} e^{i\omega_m t}). \quad (4)$$

Substituting this expression into the lattice Hamiltonian and passing to the continuum limit yields the following effective decay operator, which should be contrasted to Eq. (2):

$$H_{int} = \frac{iga^2}{\sqrt{\pi}} \sum_{m,\lambda} \int_0^1 d\xi \cos(\pi\xi) T^a_{ij}\, h^\dagger_i(\xi \mathbf{r}_{Q\overline{Q}}) \times \boldsymbol{\sigma} \cdot \hat{\mathbf{e}}_\lambda(\hat{\mathbf{r}}_{Q\overline{Q}}) (\alpha^a_{m\lambda} - \alpha^{a\dagger}_{m\lambda}) \chi_j(\xi \mathbf{r}_{Q\overline{Q}}), \quad (5)$$

where the $\hat{\mathbf{e}}(\hat{\mathbf{r}})$ are polarization vectors orthogonal to $\hat{\mathbf{r}}$. The integral is defined along the $Q\overline{Q}$ axis only. Integration over the transverse directions yields the factor a^2 which may be interpreted as the transverse size of the flux tube. Note that the phonon operators represent gluonic excitations which are perpendicular to the $Q\overline{Q}$ axis. Although this appears problematical in traditional perturbation theory, it is required here because, in the adiabatic limit, the gluonic field configuration must be defined in terms of the quark configuration and therefore the field expansion of the vector potential depends on the quark state under consideration.

The decay amplitude for a hybrid H into mesons A and B is then given by

$$\langle H|H_{int}|AB\rangle = i\frac{ga^2}{\sqrt{\pi}} \frac{2}{3} \int_0^1 d\xi \int d\mathbf{r} \cos(\pi\xi) \sqrt{\frac{2L_H+1}{4\pi}} \times e^{i\mathbf{p}\cdot\mathbf{r}/2} \varphi_H(r) \varphi^*_A(\xi\mathbf{r}) \varphi^*_B((1-\xi)\mathbf{r}) \times [\mathcal{D}^{L_H^*}_{M_L\Lambda}(\phi,\theta,-\phi) \chi^{PC}_{\Lambda,\lambda} \hat{\mathbf{e}}_\lambda(\hat{\mathbf{r}}) \cdot \langle\boldsymbol{\sigma}\rangle] \quad (6)$$

where $\langle\boldsymbol{\sigma}\rangle$ is the matrix element of the Pauli matrices between quark spin wave functions:

$$\langle\boldsymbol{\sigma}\rangle = \left\langle \frac{1}{2} s \frac{1}{2} \overline{s} \middle| S_H M_H \right\rangle \left\langle \frac{1}{2} s \frac{1}{2} \overline{s_A} \middle| S_A M_A \right\rangle \times \left\langle \frac{1}{2} s_B \frac{1}{2} \overline{s} \middle| S_B M_B \right\rangle \boldsymbol{\sigma}_{S_B \overline{S_A}}. \quad (7)$$

This amplitude should be multiplied by the appropriate flavor overlap and symmetry factor.

The evaluation of the matrix elements is greatly facilitated by performing the angular integrals analytically. This may be achieved through use of the relations $\hat{\mathbf{e}}_\Lambda(\hat{r}) = \Sigma_\lambda D^1_{\lambda\Lambda}(\phi,\theta,-\phi) \hat{\mathbf{e}}_\lambda(\hat{z})$ and

$$\hat{\mathbf{e}}_\lambda(\hat{z})\boldsymbol{\sigma}_{S_B\bar{S}_A} = -\sqrt{2}\left\langle \frac{1}{2} S_B \frac{1}{2} S_A \middle| 1\lambda \right\rangle. \tag{8}$$

The resulting expression completely factorizes from the radial and flux tube integrals except for a trivial dependence on the wave in the final channel, greatly simplifying the algebra.

We note the following general properties of the decay amplitude. The operator is nonzero only along the hybrid $Q\bar{Q}$ axis—as follows from the structure of the interaction Hamiltonian. Thus $q\bar{q}$ creation occurs on a line joining the original $Q\bar{Q}$ quarks, smeared over the transverse size of the flux tube. This is in contrast to the model of IKP which has transverse extent and a node along the $Q\bar{Q}$ axis. Furthermore the spin operator contracts with the flux tube phonon polarization vector, which is absent in the IKP model. Finally, the decay amplitude vanishes when the final mesons are identical due to the nodal structure in the vector potential. This is true for any single-phonon hybrid in an odd mode. Thus one obtains the selection rule: low-lying hybrids do not decay to identical mesons. This subsumes the selection rule of IKP so that none of their qualitative conclusions are changed. However we also predict, for example, that hybrids do not decay to pairs of identical P-wave mesons. This rule has recently been shown to be more general than specific models [10]. The preferred decay channels are to $S+P$-wave pairs [11,5]. We stress that the selection rule forbidding $S+S$-wave final states no longer operates if the internal structure or size of the two S-wave states differ [6,21].

Another rule, the ''spin selection'' rule, exists: if the $q\bar{q}$ in either hybrid or conventional mesons are in a net spin singlet configuration then decay into final states consisting only of spin singlet states is forbidden. This rule follows because pair creation is spin-triplet. It appears to be a universal feature in all non-relativistic decay models.

For $J^{PC}=1^{--}$ states this selection rule distinguishes between conventional vector mesons which are $^3S_1$ or $^3D_1$ states and hybrid vector mesons where the $q\bar{q}$ are coupled to a spin singlet. For example, it implies that in the decay of hybrid ρ_H, the channel πh_1 is forbidden whereas πa_1 is allowed; this is quite opposite to the case of $^3L_1$ conventional mesons where the πa_1 channel is relatively suppressed and πh_1 is allowed [12,13]. The extensive analysis of data in Ref. [14] revealed the clear presence of $\rho(1450)$ [15] with a strong πa_1 mode but no sign of πh_1, in accord with the hybrid situation.

There are a number of amplitudes that vanish for the SHO wave functions employed here in addition to those governed by the selection rules above. Some of these decays vanish simply due to quantum numbers, e.g. $J^{PC}=0^{-+}$ to two vector mesons (see the proof in Appendix 1 of Ref. [17]).

Some amplitudes vanish in both this work and the IKP model. These include all F-wave amplitudes for hybrid decay to two S-wave mesons, and all G-wave amplitudes. Also, 0^{-+},1^{+-} hybrid decays to two vector mesons vanishes.

In addition, the decays 2^{-+} and $1^{+-}\to 1^{+-}0^{-+}$,; $1^{++}\to 0^{++}0^{-+}$; and $0^{+-}\to 1^{++}0^{-+}$ vanish. Alternatively, in the IKP model $2^{-+}\to 1^{++}0^{-+}$ and $1^{-+}\to 2^{++}0^{-+}$ vanish.

III. HYBRID MESON WIDTHS

The final step is to calculate hybrid widths. This involves choosing prescriptions for evaluating the decay phase space, the vertex coupling ga^2, and wave function parameters.

The choice of the appropriate phase space is, unfortunately, a difficult issue to resolve (it is discussed extensively in [18]). For example, in our conventions standard relativistic phase space evaluates to

$$(\mathrm{ps}) = 2\pi k \frac{E_A E_B}{m_H} \tag{9}$$

where E_A is the energy of meson A in the final state. This can differ substantially from the nonrelativistic version:

$$(\mathrm{ps}) = 2\pi k \frac{m_A m_B}{(m_A + m_B)} \tag{10}$$

especially when pions are in the final state. Finally, we mention a third possibility employed by Kokoski and Isgur [12], called the ''mock meson'' method. The authors use

$$(\mathrm{ps}) = 2\pi k \frac{M_A M_B}{M_H} \tag{11}$$

where M_A refers to the ''mock meson'' mass of a state. This is defined to be the hyperfine-splitting averaged meson mass. In practice, the numerical result is little different from the relativistic phase space except for the case of the pion, where a mock mass of $M_\pi = 0.77\,\mathrm{GeV}$ is used. The net effect on low lying meson decays is to enhance the decay for processes with pions in the final state by a factor of M_π/E_π for each pion in the final state. This procedure improved the fit to experimental data substantially. In fact, it is generally true that the $^3P_0$ model (with relativistic phase space) fits the data quite well except for the case where pions are in the final state.

We have adopted a different approach to phase space which also solves this problem and which we believe is better physically motivated. We suggest [19] that the root of the problem lies in the Goldstone boson nature of the pion. This implies that a pion is not a simple $Q\bar{Q}$ state, but rather is collective in nature. An explicit way to incorporate this physics into a constituent quark model has been suggested by several groups [20,7]. The method relies on constructing a nontrivial vacuum for QCD which breaks chiral symmetry. The pion may then be manifested as a Goldstone mode by using the random phase approximation (RPA) to construct it. The point of interest to the current discussion is that in the random phase approximation the pion wave function contains backward moving pieces. These pieces allow new contributions to meson decay diagrams when pions are in the final state. In the chiral limit, the net result is quite simple: amplitudes with two pions in the final state should be multiplied by 3 (over the naive quark model result), while those with a single pion in the final state should be multiplied by 2. The efficacy of this prescription is illustrated in Table I.

As can be seen, the improvement is dramatic. Precisely the same argument applies to hybrid decays. Thus our pre-

TABLE I. $^3P_0$ couplings needed to reproduce experimental widths.

	$\rho\to\pi\pi$	$b_1\to\omega\pi$	$a_1\to\rho\pi$	$\pi_2\to\rho\pi$
no RPA	0.71	0.53	0.46	0.42
RPA	0.24	0.26	0.23	0.21

scription is as follows: use relativistic phase space and the RPA pion factors mentioned above to arrive at the final decay amplitudes.

The work of IKP was greatly expanded in Close and Page [21]; since one of the purposes of this work is to compare this model with IKP, we have both quoted the results of Close and Page below and have used their meson and hybrid meson wavefunction parameters as our ''standard parameters'' (these are discussed in the Appendix). Note that in order to calculate the IKP model predictions given below, we use the same normalization as in Ref. [21], which corresponds to the $^3P_0$ pair creation parameter $\gamma_0=0.39$ favored for mock meson phase space [12,18]. Although $\gamma_0=0.53$ is preferred for relativistic phase space [18], Ref. [13] used $\gamma_0=0.4$ for high mass meson resonances. We simply choose to retain $\gamma_0=0.39$.

The normalization of this model is fixed to give the same average width as the IKP model for the decays of isovector hybrids to $\eta\pi$, $\eta'\pi$ and $\rho\pi$ with the ''standard parameters.'' This yields a coupling of $ga^2=1.78\,\mathrm{GeV}^{-2}$. These particular decay modes were chosen because the two models can analytically be shown to mimic the predictions of each other in decays to two ground state or radially excited S-wave final states. Thus decays to these final states may be regarded as ''model invariant.'' Finally, as discussed above, we note that the absolute widths in the IKP model could be up to $(0.53/0.39)^2\approx 2$ times bigger than the widths quoted here. Furthermore, since phase space conventions and absolute magnitude conventions have changed since former IKP model calculations [21] care should be taken with comparisons. Indeed, the authors of IKP state that a model error of (an additional) factor of 2 should be allowed for in their predicted widths.

To make contact with the original development of this model [6] and to illustrate the parameter dependence of the model predictions, we also employ the parameters of Ref. [6] as an ''alternative parameter'' set. This set was normalized to the experimental decay pattern of the hybrid meson candidate $\pi(1800)$, yielding[1] $ga^2=1.28\,\mathrm{GeV}^{-2}$. These parameters are also listed in the Appendix.

Simple harmonic oscillator (SHO) wave functions are used throughout for the final state mesons. This is typical of decay calculations and it has been demonstrated that using Coulomb+linear wave functions does not change the results significantly [18,12]. We have taken the following masses for the $u\bar{u}$, $s\bar{s}$, $c\bar{c}$, and $b\bar{b}$ hybrids: 1.8, 2.0, 4.1, and 10.7 GeV respectively. Masses for known mesons are taken from Ref. [15] and otherwise from Ref. [38]. The quark model assignments for the mesons are those of the Particle Data Group (PDG) tables [15]. The $f_0(1370)$ is assumed to be the scalar $(1/\sqrt{2})(u\bar{u}+d\bar{d})$ state. We assume the $J^{PC}=2^{++}$, 1^{++},0^{++},1^{+-} $s\bar{s}$ mesons to be $f_2'(1525)$,$f_1(1510)$, $f_0(1370)$,$h_1(1380)$ respectively. Thus $f_0(1370)$ denotes a generic scalar state at 1.37 GeV, containing either light quarks or $s\bar{s}$, depending on the context.

The flavor structure of the η is taken to be $\sqrt{\frac{1}{2}}(\sqrt{\frac{1}{2}}(u\bar{u}+d\bar{d})-s\bar{s})$ at 547 MeV and η' is $\sqrt{\frac{1}{2}}(\sqrt{\frac{1}{2}}(u\bar{u}+d\bar{d})+s\bar{s})$ at 958 MeV. The $\eta_u(1295)$ and $\eta_s(1490)$ are assumed to be $\sqrt{\frac{1}{2}}(u\bar{u}+d\bar{d})$ and $s\bar{s}$ respectively, with $\eta_s(1490)$ the second $\eta(1440)$ peak at 1490 MeV. $K(1460)$ is not well established. $D^{**}(2^+)$ denotes the PDG state $D_2^*(2460)$. $D^{**}(1_L^+)$ and $D^{**}(1_H^+)$ are the low and high mass 1^+ states respectively. The high mass state can be identified with the PDG state $D_1(2420)$.

As stated earlier, we employ relativistic phase space and RPA pion phase space factors. We also extend the RPA prescription to kaons and ηs; but not to the η'. Decay modes include all possible charge combinations, e.g. $\rho\pi$ means $\rho^+\pi^-$, $\rho^0\pi^0$ and $\rho^-\pi^+$ for isoscalar decay.

In the following tables we present the dominant widths for hybrid $H\to AB$ for various J^{PC} hybrids in partial wave L. Column 1 indicates the J^{PC} of the hybrid, column 2 the decay mode and column 3, L. In columns 4, 5, 6 and 8 we indicate predictions of this model. Column 6 uses the ''standard parameters'' used throughout the text and defined in the Appendix. Column 5 uses the same parameters, except that all hybrids are assumed to be 0.2 GeV heavier (and the $c\bar{c}$ hybrids 0.3 GeV heavier to put them above the $D^{**}D$ thresholds at approximately 4.3 GeV). All calculations are made in the narrow resonance approximation. The effects of this approximation may be estimated by comparing the predictions of columns 5 and 6. Column 4 uses the ''alternative parameters.'' Columns 4 and 6 should hence be compared to estimate parameter sensitivity of our predictions. For hybrid decays to two ground state S-wave mesons we indicate the ''reduced width'' in column 8. This is the width divided by the dimensionless ratio $(\beta_A^2-\beta_B^2)^2/(\beta_A^2+\beta_B^2)^2$, where β is the inverse radius of the SHO wave function [21]. It gives a measure of how strong the decay is with the difference of the wave functions explicitly removed. In column 7 we give IKP model predictions for the ''standard parameters,'' so that columns 6 and 7 should be compared when this model is compared with the IKP model.

As stated earlier, we omit F-wave amplitudes for hybrid to two S-wave mesons, and all G-wave amplitudes, since these vanish in both models. We do not list decays with two S-wave mesons in the final state which have identical wave functions (e.g. $\pi\pi$, $\rho\rho$), since these amplitudes vanish due to the ''S+S'' selection rule. The symbol ''$\varnothing$'' indicates that an amplitude is exactly zero, not only numerically small. Finally, a dash indicates that a decay mode is below threshold. Note that the predicted total widths given below are lower bounds. This is predominantly due to three body decay

[1]Note that Ref. [6] did not use the RPA pion prescription. The value of the coupling quoted here corrects this. None of the results of that paper change.

modes which we have neglected such as $X\sigma$, $Xf_0(980)$, or $Xa_0(980)$ (it is widely believed that the σ is a $\pi\pi$ correlation while the f_0 and a_0 may be $K\bar{K}$ bound states). These modes are problematic because the specified states do not appear to be simple $q\bar{q}$ states and therefore are difficult to incorporate into our decay model.

IV. DISCUSSION

We proceed to discuss the phenomenology of mainly isovector hybrids made from u,d flavored quarks for each J^{PC}, as these are expected to be the easiest to isolate experimentally.

A. Light hybrids

1. 1^{--}

It was argued in Refs. [13, 22] that the $\rho(1450)$ and the $\omega(1420)/\omega(1600)$ cannot be accommodated within the phenomenologically successful $^3P_0$ decay model as conventional mesons—a hybrid component is needed. This conclusion depends strongly on the results of the influential data analysis of Ref. [14]. The central problem is that the substantial experimental $a_1\pi$ mode [14] cannot be accommodated along with other modes of $\rho(1450)$ if the state is $2\,^3S_1$ or $^3D_1$ quarkonium. However, if the experimental $a_1\pi$ width of 190 MeV [14] can be reduced by 50%, the $\rho(1450)$ can be fitted as $2\,^3S_1$ $q\bar{q}$ [22]. The IKP model predicted that $a_1\pi$ would be the largest decay mode of a hybrid, consistent with the data. It is of interest to examine these conclusions here.

For a hybrid isovector 1^{--} at 1.5 GeV we calculate for ''standard parameters'' the widths

	$\omega\pi$	$\rho\eta$	K^*K	$a_1\pi$	
this work	6	2	.6	15	MeV
IKP model	5	1	.3	43	MeV

where both models predict $\pi\pi$, $\rho\rho$, KK, $h_1\pi$ and $a_2\pi$ to vanish. For a hybrid isoscalar at 1.5 GeV

	$\rho\pi$	$\omega\eta$	K^*K	
this work	20	1	.6	MeV
IKP model	17	1	.3	MeV

where both models predict KK and $b_1\pi$ to be negligible.

The predictions for the models are very similar, except that the $a_1\pi$ mode of the isovector state is smaller in this model. However, the ordering of modes according to their relative sizes remains the same, and $a_1\pi$ remains the dominant channel. It is clear that it becomes difficult to support the huge experimental $a_1\pi$ mode in both models. In the light of this we urge quantification of this mode at DAΦNE and JLab (and at a coupled channel analysis currently in progress at Crystal Barrel [23]).

If the $\rho(1450)$ has indicated the existence of the vector hybrid nonet, then we need to establish which of the other seven multiplets expected nearby should also be visible. States whose couplings are predicted to be strong, with highly visible decay channels and moderate widths relative to the ρ candidate, *must* be seen if hybrids are to be established. Conversely, channels where no signals are seen should be those with signals which are predicted to be weak.

2. 0^{+-}

The clearest signature for a hybrid meson is the appearance of a flavored state with exotic J^{PC}. It was noted in the IKP model [21] that the isovector 0^{+-} width is predicted to be large (over 600 MeV according to Table II). Here the width is 100–250 MeV depending on parameters, making the state narrower. However, as shown in Table II, if the mass of the state increases, the width may increase dramatically. There are accordingly two likely reasons why this state has not yet been observed: (i) Its mass is higher than 1.8 GeV, making it very wide. This possibility is underpinned by recent lattice gauge theory calculations supporting a mass difference of $\sim 0.2 \pm 0.2$ GeV between 0^{+-} and the lowest lying 1^{-+} hybrid [1]. (ii) Its decay modes are idiosyncratic. It can be seen from the table that decays are only to $S+P$-wave states, most likely to $\pi(1300)\pi$, $a_1\pi$ and $h_1\pi$. However, $\pi(1300)$, a_1, and h_1 are broad states, making the 0^{+-} difficult to isolate.

3. 2^{+-}

The isovector 2^{+-} was predicted to be broad in the IKP model (~ 250 MeV) [21]. This is especially true if the mass of the state increases, as indicated by lattice gauge theory calculations, which suggest a mass difference of $\sim 0.7 \pm 0.3$ GeV between 2^{+-} and 1^{-+} levels [1]. However, in this model we discover a radically different result: 2^{+-} is ~ 5 MeV wide and rises to only ~ 10 MeV at 2 GeV. The total width of the 2^{+-} hence forms a strong test for the model. Part of the difficulty to detect the 2^{+-} may be that decays to $S+S$-wave states only occur in D-wave, and that decay modes like $a_2\pi$, $a_1\pi$ and $h_1\pi$ contain broad P-wave states. However, in view of the possible narrowness of this state, we urge experimenters to allow for the exotic 2^{+-} wave in partial wave analyses. Particularly, $a_2\pi \to (\rho\pi)\pi \to 4\pi$ should be studied.

4. 1^{-+}

An excellent opportunity for isolating exotic hybrids occurs in the 1^{-+} wave. Recently, there has been several experimental claims for 1^{-+} signals, most notably by Brookhaven and VES, in two distinct mass regions: (i) Refs. [24,25] sees a broad structure in the mass region 1.6–2.2 GeV in $f_1\pi$, which is suggestive of being a composite of two objects at 1.7 and 2.0 GeV. It is the latter that appears to have a resonant phase though they admit that more data is required for a firm conclusion. (ii) Reference [26] claims a resonance at 1593 ± 8 MeV with width 168 ± 20 MeV and Ref. [27] a ''preliminary'' resonance at 1.62 ± 0.02 GeV with width 0.24 ± 0.05 GeV. We hence study model predictions for 1^{-+} states at 1.6 and 2.0 GeV.

Our expectations for a $J^{PC}=1^{-+}$ hybrid at 2.0 GeV are (in MeV)

TABLE II. 1.8 GeV isovector hybrid decay modes (MeV).

			alt	2.0 GeV hybrid	standard	IKP	reduced
2^{-+}	$\rho\pi$	P	9	16	13	12	57
	K^*K	P	1	5	2	1	17
	$\rho\omega$	P	0	0	0	0	20
	$f_2(1270)\pi$	S	19	10	9	14	
		D	.1	.2	.05	11	
	$f_1(1285)\pi$	D	.1	.3	.06	∅	
	$f_0(1370)\pi$	D	.02	.08	.01	.6	
	$b_1(1235)\pi$	D	∅	∅	∅	20	
	$a_2(1320)\eta$	S	–	7	–	–	
		D	–	.01	–	–	
	$a_1(1260)\eta$	D	0	.05	0	0	
	$a_0(1450)\eta$	D	–	0	–	–	
	$K_2^*(1430)K$	S	–	11	–	–	
		D	–	0	–	–	
	$K_1(1270)K$	D	0	.01	0	.02	
	$K_0^*(1430)K$	D	–	0	–	–	
	$K_1(1400)K$	D	–	0	–	–	
	$\rho(1450)\pi$	P	.8	12	3	2	
	$K^*(1410)K$	P	–	1	–	–	
	Γ (MeV)		30	63	27	59	
1^{-+}	$\eta\pi$	P	0	.02	.02	.02	99
	$\eta'\pi$	P	0	.01	.01	0	30
	$\rho\pi$	P	9	16	13	12	57
	K^*K	P	1	5	2	1	17
	$\rho\omega$	P	0	0	0	0	13
	$f_2(1270)\pi$	D	.2	.5	.1	∅	
	$f_1(1285)\pi$	S	18	10	9	14	
		D	.06	.2	.04	7	
	$b_1(1235)\pi$	S	78	40	37	51	
		D	2	3	1	11	
	$a_2(1320)\eta$	D	–	.02	–	–	
	$a_1(1260)\eta$	S	5	7	3	8	
		D	0	.01	0	.01	
	$K_2^*(1430)K$	D	–	0	–	–	
	$K_1(1270)K$	S	4	7	2	6	
		D	0	.2	0	.04	
	$K_1(1400)K$	S	–	33	–	–	
		D	–	0	–	–	
	$\pi(1300)\eta$	P	–	5	–	–	
	$\eta_u(1295)\pi$	P	3	27	11	8	
	$K(1460)K$	P	–	.8	–	–	
	$\rho(1450)\pi$	P	.8	12	3	2	
	$K^*(1410)K$	P	–	1	–	–	
	Γ (MeV)		121	168	81	117	
1^{--}	$\omega\pi$	P	9	16	13	12	57
	$\rho\eta$	P	4	9	6	4	30
	$\rho\eta'$	P	.1	1	.2	.1	1
	K^*K	P	3	9	5	3	34
	$a_2(1320)\pi$	D	.5	2	.3	16	
	$a_1(1260)\pi$	S	78	41	37	51	
		D	.4	.8	.2	11	
	$h_1(1170)\pi$	S			∅		

TABLE II. (*Continued*).

			alt	2.0 GeV hybrid	standard	IKP	reduced
		D			∅		
	$b_1(1235)\eta$	S			∅		
		D			∅		
	$K_2^*(1430)K$	D	–	0	–	–	
	$K_1(1270)K$	S	6	12	4	11	
		D	0	.01	0	0	
	$K_1(1400)K$	S	–	17	–	–	
		D	–	0	–	–	
	$\omega(1420)\pi$	P	1	14	4	4	
	$K^*(1410)K$	P	–	3	–	–	
	Γ (MeV)		103	121	70	112	
2^{+-}	$\omega\pi$	D	.5	1	1	1	4
	$\rho\eta$	D	.1	.6	.2	.1	1
	$\rho\eta'$	D	0	.02	0	0	0
	K^*K	D	.04	.2	.08	.04	.6
	$a_2(1320)\pi$	P	.7	.9	.4	130	
		F	0	.02	0	.2	
	$a_1(1260)\pi$	P	3	4	2	45	
		F	.01	.02	0	.3	
	$h_1(1170)\pi$	P	2	2	1	69	
		F	.01	.03	.01	.5	
	$b_1(1235)\eta$	P	.02	.5	.01	.8	
		F	0	0	0	0	
	$K_2^*(1430)K$	P	–	.04	–	–	
		F	–	0	–	–	
	$K_1(1270)K$	P	0	.03	0	.6	
		F	0	0	0	0	
	$K_1(1400)K$	P	–	.3	–	–	
		F	–	0	–	–	
	$\pi(1300)\pi$	D	.08	1	.2	.2	
	$\omega(1420)\pi$	D	.02	.4	.04	.04	
	$K^*(1410)K$	D	–	.01	–	–	
	Γ (MeV)		7	11	5	248	
0^{-+}	$\rho\pi$	P	37	63	51	47	230
	K^*K	P	5	18	10	5	69
	$\rho\omega$	P			∅		
	$f_2(1270)\pi$	D	1	3	.6	8	
	$f_0(1370)\pi$	S	62	40	30	62	
	$a_2(1320)\eta$	D	–	.1	–	–	
	$a_0(1450)\eta$	S	–	4	–	–	
	$K_2^*(1430)K$	D	–	.02	–	–	
	$K_0^*(1430)K$	S	–	44	–	–	
	$\rho(1450)\pi$	P	3	47	10	10	
	$K^*(1410)K$	P	–	5	–	–	
	Γ (MeV)		108	224	102	132	
1^{+-}	$\omega\pi$	S	23	19	26	38	118
		D	.3	.8	.4	.3	2
	$\rho\eta$	S	15	21	25	22	118
		D	.07	.3	.1	.06	.6
	$\rho\eta'$	S	3	8	5	4	25
		D	0	.01	0	0	0

TABLE II. (*Continued*).

			alt	2.0 GeV hybrid	standard	IKP	reduced
	K^*K	S	27	52	47	36	339
		D	.02	.1	.04	.02	.3
	$a_2(1320)\pi$	P	19	26	10	49	
		F	0	.02	0	.1	
	$a_1(1260)\pi$	P	9	10	5	29	
	$a_0(1450)\pi$	P	3	6	1	26	
	$h_1(1170)\pi$	P	∅	∅	∅	95	
	$b_1(1235)\eta$	P	∅	∅	∅	1	
	$K_2^*(1430)K$	P	–	1	–	–	
		F	–	0	–	–	
	$K_1(1270)K$	P	.04	.6	.02	5	
	$K_0^*(1430)K$	P	–	.4	–	–	
	$K_1(1400)K$	P	–	.4	–	–	
	$\omega(1420)\pi$	S	16	82	58	79	
		D	.01	.2	.02	.02	
	$K^*(1410)K$	S	–	110	–	–	
		D	–	.01	–	–	
	Γ (MeV)		115	338	177	384	
0^{+-}	$a_1(1260)\pi$	P	∅	∅	∅	309	
	$h_1(1170)\pi$	P	47	45	24	37	
	$b_1(1235)\eta$	P	.6	12	.4	.3	
	$K_1(1270)K$	P	.7	10	.4	7	
	$K_1(1400)K$	P	–	1	–	–	
	$\pi(1300)\pi$	S	60	246	222	312	
	$K(1460)K$	S	–	115	–	–	
	Γ (MeV)		108	429	247	665	
1^{++}	$\rho\pi$	S	23	19	26	38	116
		D	1	3	2	1	8
	K^*K	S	14	26	24	18	170
		D	.04	.3	.09	.04	.6
	$\rho\omega$	S	0	0	0	0	47
		D	0	0	0	0	.03
	$f_2(1270)\pi$	P	4	5	2	75	
		F	.01	.03	0	.3	
	$f_1(1285)\pi$	P	7	9	4	62	
	$f_0(1370)\pi$	P	∅	∅	∅	4	
	$b_1(1235)\pi$	P	∅	∅	∅		
	$a_2(1320)\eta$	P	–	.9	–	–	
		F	–	0	–	–	
	$a_1(1260)\eta$	P	.2	3	.09	1	
	$a_0(1450)\eta$	P	–	∅	–	–	
	$K_2^*(1430)K$	P	–	.4	–	–	
		F	–	0	–	–	
	$K_1(1270)K$	P	.07	1	.05	1	
	$K_0^*(1430)K$	P	–	0	–	–	
	$K_1(1400)K$	P	–	.7	–	–	
	$\rho(1450)\pi$	S	14	80	50	66	
		D	.02	.6	.05	.04	
	$K^*(1410)K$	S	–	55	–	–	
		D	–	.01	–	–	
	Γ (MeV)		63	204	108	269	

	$b_1\pi$	$K_1(1400)K$	$\eta(1295)\pi$	$\rho\pi$	$\rho(1450)\pi$	$f_1\pi$	$a_1\eta$	$K_1(1270)K$
this work	43	33	27	16	12	10	7	7
IKP model	58	75	21	16	12	38	13	19

where we have neglected K^*K, $f_2\pi$, $\pi(1300)\eta$, $K(1460)K$, and $K^*(1410)K$ modes which are predicted to be smaller than 5 MeV in both models. Furthermore, the $\eta\pi$, $\eta'\pi$, $\rho\omega$, $a_2\eta$, and $K_2^*(1430)K$ modes are all negligible in both models. Because of the substantially increased phase space available relative to a 1.6 GeV hybrid candidate, $P+S$ channels are dominant. The model has several modes suppressed relative to the IKP model. Also note in addition to the important $b_1\pi$ channel, $K_1(1400)K$ emerges as prominent channel, leading us to suggest the search channel $KK\pi\pi$.

For a 1^{-+} hybrid at 1.6 GeV one has

	$b_1\pi$	$\rho\pi$	$f_1\pi$	$\eta(1295)\pi$	K^*K	
this work	24	9	5	2	.8	MeV
IKP model	59	8	14	1	.4	MeV

where both models predict $\eta\pi$, $\eta'\pi$, $\rho\omega$ and $f_2\pi$ to be 0 MeV. Superficially, the main effect of this model is to make the $P+S$ modes of a more similar size to the $S+S$ modes than they are in the IKP model, in agreement with the clear presence of the experimental state in $\rho\pi$ [24]. However, this conclusion is parameter dependent (compare columns 4 and 6 in Table II). Nevertheless we emphasize the importance of searching for the hybrid in $\rho\pi$, as well as in the $b_1\pi$ and $f_1\pi$ channels. Also, both models concur that $b_1\pi$ should be primarily focused upon. Such a search has been proposed and conditionally approved at JLab [28]. Although both models underpredict the total experimental width at $\sim 50-100$ MeV, we do not consider this significant at the level of accuracy expected of this model, especially in view of the fact that not all possible decay modes have been calculated.

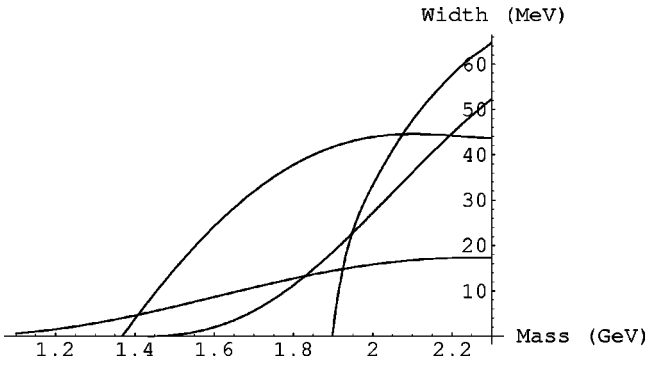

FIG. 1. Dominant partial widths of a 1^{-+} isovector hybrid at various hybrid masses. The partial widths to $K_1(1400)K$, $\eta(1295)\pi$, $b_1\pi$ and $\rho\pi$ correspond to the highest to the lowest intersections with the vertical axis.

The strong dependence of the partial widths on the hybrid mass is displayed in Fig. 1. Note that the ''S+P'' selection rule forces this to be true for any hybrids in the 2 GeV mass range because decays may only occur to final states near threshold.

It is significant that there is no experimental evidence for hybrids in the 1.6–2 GeV region in $\eta\pi$ [29] which is consistent with the predictions of both models, and is in fact model-independent due to a relativistic symmetrization selection rule [16]. In this context, searches in $\eta\pi$ at JLab and BNL [30,29] could be disappointing.

More experimental work is needed to clearly establish whether both 1^{-+} signals are solid, and more detailed knowledge of branching ratios are necessary in order to compare our predictions with experiment.

5. 1^{++}

An important model distinction emerges for 1^{++} hybrids: we predict widths of approximately 100 MeV, while the IKP model predicts widths larger than 200 MeV. We shall argue below that the experimental evidence for the $a_1(1700)$ indicates that if it is regarded as a single resonance, then it is not a 1^{++} hybrid. Within this model *either* both the conventional meson and the hybrid are produced, with the hybrid weaker, *or* the 1^{++} hybrid is higher than 2 GeV in mass, which would push its width to more than 200 MeV. In either case we expect the dominant decay channel in this model to be to $1^{++}\to\rho\pi\to 3\pi$ or $1^{++}\to\rho(1450)\pi\to 5\pi$ [and if phase space allows $K^*(1410)K$]. Another experimental challenge would be considering the possibility of two resonances in the 1.6–2 GeV mass region.

We now argue that the experimental evidence for the $a_1(1700)$ is consistent with it being a conventional meson. Here we assume for simplicity that the $a_1(1700)$ is a single resonance, independent of the channel it is observed in. Current experimental data does not allow us to go beyond this assumption. It was noted in Ref. [13] that the large D-wave to S-wave ratio for $\rho\pi$ amplitudes found by VES is consistent with expectations for a $2\,^3P_1$ conventional meson. It is clear from Table II that the large D-wave is not explicable for a hybrid in this model or in the IKP model. Reference [13] also predicted a $\rho\pi$ width of 57 MeV for $2\,^3P_1$, while we expect a $\rho\pi$ width of 30 MeV for a 1.7 GeV state. This is consistent with the $2\,^3P_1$ being strongly produced via the $\rho\pi$ production vertex sampled at VES. This, together with the stronger $f_1\pi$ width of the $2\,^3P_1$ (18 MeV), is consistent with the state observed in $f_1\pi$ [24,25] being the $2\,^3P_1$. VES also reported possible evidence for the $f_0(1370)\pi$ mode. Since the predicted $f_0(1370)\pi$ width of $2\,^3P_1$ quarkonium is 2 MeV and that of a hybrid is 0 MeV, this supports the weakness of the mode observed. Recently, VES has reported the

observation of a structure in $\omega\pi^+\pi^-$ at 1.8 GeV that can be identified with the $a_1(1700)$, coupling to the $b_1\pi$ and $\rho\omega$ channels [25]. In both the current model and the IKP model, this is inconsistent with the hybrid interpretation, as the coupling of the hybrid to $b_1\pi$ and $\rho\omega$ is expected to vanish. In fact, VES reports an absence of $\rho\omega$ S-wave [31], inconsistent with the hybrid interpretation where the S-wave dominates the D-wave (see Table II), but consistent with the $^3P_0$ model prediction that the S-wave should be zero [see Eq. (A53) of Ref. [13]]. Moreover, the $f_1\pi$ channel is dramatically suppressed for the hybrid in this model in contrast to the IKP model. In summary, if we assume that $a_1(1700)$ is a single resonance, it is consistent with being a conventional meson. Within this assumption, it should be counted as one of the successes of this approach that we can explain the nonobservation of the 1^{++} hybrid in a way the IKP model cannot.

6. 0^{-+}

It is clear from Table II that the predictions of this model and the IKP model are very similar, except for $f_0(1370)\pi$ which can vary substantially depending on parameters. References [13,22] concluded that the $\pi(1800)$ cannot be understood as a conventional meson in the $^3P_0$ model. References [21,32] concluded that the $\pi(1800)$ can be interpreted as a hybrid meson in the IKP model. The current work does not change these conclusions. Reference [6] contains a calculation of the widths of the $\pi(1800)$ in this model which include below threshold decays to $K_0^*(1430)K$ of 85 MeV.[2] It is useful to correlate the decay modes to experimentally known ratios. Specifically, using the VES experimental branching ratios[3] [33] and correcting for decays of particles into the specific channels observed by VES [34], we obtain

	$K_0^*(1430)K$	$f_0(1370)\pi$	$\rho\pi$	K^*K	$\rho\omega$
Experiment	1.0 ± 0.3	0.9 ± 0.3	<0.36	<0.06	0.4 ± 0.2
this work	<0.7	0.6	0.31	0.05	0

where the model widths evaluated for the ''alternative parameters'' have been scaled by a common factor to allow comparison to the experimental ratios deduced in Ref. [34]. The correspondence is remarkable.

We emphasize that although $\rho\pi$ is suppressed in the data, we expect the resonance to have a non-negligible coupling to this channel. The total width is expected to be $\Gamma_{total}\sim 100-150$ MeV and is consistent with the experimental width, since the decay modes $f_0(1500)\pi$, $f_0(980)\pi$ and $a_0(980)\eta$ that are known to occur [35,36] have not been computed here and are experimentally known to give substantial additional contributions [34].

One inconsistency with VES data is the $\rho\omega$ mode. It is significant that the resonance in $\rho\omega$ has a mass 1.732 ± 0.01 GeV, shifted significantly downward from the usual $\pi(1800)$ mass parameters, and that there are indications of the presence of a broad 0^{-+} wave [37]. This may signal the presence of $3\ ^1S_0$ light quark state expected at 1.88 GeV [38] with dominant decay to $\rho\omega$ [13,22], removing the apparent inconsistency with the hybrid interpretation of $\pi(1800)$.

Important tests are now that there should be a measurable coupling to the $\rho\pi$ channel with only a small $f_2\pi$ or K^*K contribution.

7. 2^{-+}

We expect both isovector and isoscalar 2^{-+} hybrids to be narrow, and they should hence be seen. The difference between the predictions of our approach and the IKP model does not appear to be substantial, especially when parameters are allowed to vary (see Table II). The most striking difference between the models is the isovector 2^{-+} decay to $b_1\pi$, which this model finds exactly zero. However, it is fairly small in the IKP model too. From the selection rule forbidding the decay of a spin singlet meson into pairs of spin singlets, it follows that the decay of $^1D_2(Q\bar{Q})\to b_1\pi$ is prevented. Hence the $b_1\pi$ channel may not be a strong discriminant between hybrid and conventional 2^{-+}, as previously suggested [13,21]. Recent VES data on the 2^{-+} in $b_1\pi$ does appear to indicate a structure at 1.8 GeV, but no firm conclusions are possible at this stage [25]. The phenomenology of the 2^{-+} discussed in Refs. [21,13] suffices at this stage: isovector decays to $\rho\pi$ and $f_2\pi$ and isoscalar decays to $a_2\pi$ remains the dominant signature.

VES noted a 2^{-+} structure $\pi_2(2100)$ at 2.09 ± 0.03 GeV with width 520 ± 100 MeV coupling strongly to $f_0(1370)\pi$ but absent in $f_2\pi$ and $f_0(980)$ [36], although an earlier experiment by ACCMOR reported the state in $\rho\pi$, $f_2\pi$ and $f_0(1370)\pi$ [15]. A similar excess may exist in E852 data [26]. Theory expects a second radially excited quarkonium state at 2.13 GeV [38].

In the isoscalar sector, evidence exists for a 2^{-+} resonance at ~1.8 GeV. There are three plausible possibilities

[2]Some of the $K_0^*(1430)K$ mode predicted in this model is expected to couple to $f_0(980)\pi$ via $K_0^*(1430)K\to(K\pi)K\to f_0(980)\pi$ final state interactions, which are known to be substantial experimentally, so that this model estimate is actually less than 85 MeV.

[3]The experimentally measured $KK\pi$ in S-wave is assumed to arise solely from $K_0^*(1430)K$.

TABLE III. 1.8 GeV isoscalar hybrid decay modes (MeV).

			alt	2.0 GeV hybrid	standard	IKP	reduced
2^{-+}	K^*K	P	1	5	2	1	17
	$a_2(1320)\pi$	S	52	31	25	45	
		D	.2	.6	.1	22	
	$a_1(1260)\pi$	D	.5	1	.3	∅	
	$a_0(1450)\pi$	D	.02	.1	.01	.6	
	$f_2(1270)\eta$	S	–	8	–	–	
		D	–	.02	–	–	
	$f_1(1285)\eta$	D	–	.02	–	–	
	$f_0(1370)\eta$	D	–	0	–	–	
	$K_2^*(1430)K$	S	–	11	–	–	
		D	–	0	–	–	
		G	–	0	–	–	
	$K_1(1270)K$	D	0	.01	0	0	
	$K_0^*(1430)K$	D	–	0	–	–	
	$K_1(1400)K$	D	–	0	–	–	
	$K^*(1410)K$	P	–	1	–	–	
	Γ (MeV)		54	58	27	69	
1^{-+}	$\eta'\eta$	P	0	0	0	0	10
	K^*K	P	1	5	2	1	17
	$a_2(1320)\pi$	D	.4	1	.2	∅	
	$a_1(1260)\pi$	S	59	30	28	38	
		D	.3	.6	.2	34	
	$f_2(1270)\eta$	D	–	.05	–	–	
	$f_1(1285)\eta$	S	–	8	–	–	
		D	–	.01	–	–	
	$K_2^*(1430)K$	D	–	0	–	–	
	$K_1(1270)K$	S	4	7	2	7	
		D	0	.2	0	0	
	$K_1(1400)K$	S	–	33	–	–	
		D	–	0	–	–	
	$\pi(1300)\pi$	P	8	65	27	27	
	$\eta_u(1295)\eta$	P	–	6	–	–	
	$K(1460)K$	P	–	.8	–	–	
	$K^*(1410)K$	P	–	1	–	–	
	Γ (MeV)		73	158	59	107	
0^{-+}	K^*K	P	5	18	10	5	69
	$a_2(1320)\pi$	D	2	6	1	16	
	$a_0(1450)\pi$	S	145	114	70	175	
	$f_2(1270)\eta$	D	–	.2	–	–	
	$f_0(1370)\eta$	S	–	23	–	–	
	$K_2^*(1430)K$	D	–	.02	–	–	
	$K_0^*(1430)K$	S	–	44	–	–	
	$K^*(1410)K$	P		5			
	Γ (MeV)		152	210	81	196	
1^{--}	$\rho\pi$	P	28	47	38	35	172
	$\omega\eta$	P	3	9	6	4	29
	$\omega\eta'$	P	.1	1	.2	.3	.8
	K^*K	P	3	9	5	3	35
	$b_1(1235)\pi$	S	∅	∅	∅		
		D			∅		
	$h_1(1170)\eta$	S			∅		

TABLE III. (*Continued*).

			alt	2.0 GeV hybrid	standard	IKP	reduced
	$K_2^*(1430)K$	D	–	0	–	–	
	$K_1(1270)K$	S	6	12	4	11	
		D	0	.01	0	0	
	$K_1(1400)K$	S	–	17	–	–	
		D	–	0	–	–	
	$\rho(1450)\pi$	P	2	35	8	7	
	$\omega(1420)\eta$	P	–	.6	–	–	
	$K^*(1410)K$	P	–	3	–	–	
	Γ (MeV)		42	134	61	60	
2^{+-}	$\rho\pi$	D	1	4	2	2	11
	$\omega\eta$	D	.1	.5	.2	.1	1
	$\omega\eta'$	D	0	.03	0	0	0
	K^*K	D	.04	.2	.08	.04	.6
	$b_1(1235)\pi$	P	4	5	2	164	
		F	.02	.07	.01	.8	
	$h_1(1170)\eta$	P	.2	.7	.1	6	
	$K_2^*(1430)K$	P	–	.04	–	–	
		F	–	0	–	–	
	$K_1(1270)K$	P	0	.03	0	.6	
		F	0	0	0	0	
	$K_1(1400)K$	P	–	.3	–	–	
		F	–	0	–	–	
	$\rho(1450)\pi$	D	.02	.8	.06	.05	
	$\omega(1420)\eta$	D	–	0	–	–	
	$K^*(1410)K$	D	–	.01	–	–	
	Γ (MeV)		5	12	4	166	
1^{+-}	$\rho\pi$	S	70	57	77	114	350
		D	.8	2	1	1	6
	$\omega\eta$	S	15	22	25	22	119
		D	.07	.3	.1	.06	.6
	$\omega\eta'$	S	4	8	5	15	24
		D	0	.02	0	0	0
	K^*K	S	27	52	47	36	339
		D	.02	.1	.04	.02	.3
	$b_1(1235)\pi$	P	∅	∅	∅	231	
	$h_1(1170)\eta$	P	∅	∅	∅	9	
	$K_2^*(1430)K$	P	–	1	–	–	
		F	–	0	–	–	
	$K_1(1270)K$	P	.04	.6	.02	5	
	$K_0^*(1430)K$	P	–	.4	–	–	
	$K_1(1400)K$	P	–	.4	–	–	
	$\rho(1450)\pi$	S	42	240	150	199	
		D	.01	.4	.04	.03	
	$\omega(1420)\eta$	S	–	38	–	–	
		D	–	0	–	–	
	$K^*(1410)K$	S	–	110	–	–	
		D	–	.01	–	–	
	Γ (MeV)		158	529	305	632	
0^{+-}	$b_1(1235)\pi$	P	110	119	56	85	
	$h_1(1170)\eta$	P	4	17	3	2	
	$K_1(1270)K$	P	.7	10	.4	7	

TABLE III. (*Continued*).

			alt	2.0 GeV hybrid	standard	IKP	reduced
	$K_1(1400)K$	P	–	1	–	–	
	$K(1460)K$	S	–	115	–	–	
	Γ (MeV)		115	262	59	94	
1^{++}	K^*K	S	17	26	24	18	170
		D	.04	.3	.09	.04	.6
	$a_2(1320)\pi$	P	10	14	5	179	
		F	.01	.06	.01	.4	
	$a_1(1260)\pi$	P	28	30	14	232	
	$a_0(1450)\pi$	P	$\varnothing$	$\varnothing$	$\varnothing$	6	
	$f_2(1270)\eta$	P	–	1	–	–	
		F	–	0	–	–	
	$f_1(1285)\eta$	P	–	2	–	–	
	$f_0(1370)\eta$	P	$\varnothing$	$\varnothing$	$\varnothing$	–	
	$K_2^*(1430)K$	P	–	.4	–	–	
		F	–	0	–	–	
	$K_1(1270)K$	P	.07	1	.05	1	
	$K_0^*(1430)K$	P	–	0	–	–	
	$K_1(1400)K$	P	–	.7	–	–	
	$K^*(1410)K$	S	–	55	–	–	
		D	–	.01	–	–	
	Γ (MeV)		55	130	43	436	

for its interpretation as a conventional quarkonium state:

(i) Light quark $^1D_2$: The light quark $^1D_2$ state $\eta_2(1645)$ has most likely already been isolated by Crystal Barrel [39,40] and WA102 [41], as interpreted in Ref. [13].

(ii) $s\bar{s}\,^1D_2$: This would be a natural assignment for a $\sim$1.8 GeV state, based on the predicted mass of 1.89 GeV [38]. However, this assignment appears troublesome if we consider the fact that it has only been observed in final states not[4] containing strangeness. Moreover, there is evidence from Crystal Ball and CELLO for an isovector partner at $\sim$1.8 GeV (see the detailed discussion in Ref. [13]), in contradiction with the $s\bar{s}$ assignment. However, the isovector partner is not seen in recent analyses from ARGUS [43] and L3 [44]. It is expected that E852 would have more to contribute on this subject in the $\rho\pi$ [26], $f_1\pi$ and $a_2\eta$ channels [45].

(iii) Light quark $2\,^1D_2$: As observed above, these states are expected at much higher masses than $\sim$1.8 GeV, and there is already evidence for an isovector 2^{-+} in the correct mass region.

If future experimental work determines that none of these three possibilities are viable interpretations for the 1.8 GeV state, there is a strong possibility that the $\sim$1.8 GeV isoscalar state is a hybrid meson. This is because it is unlikely to be a glueball which is predicted by lattice gauge theory at 3.0 $\pm$0.2 GeV [46]. We also do not expect a molecule or four-quark state in this region, although the state may contain a long range $f_2\eta$ component due to its nearness to the $f_2\eta$ threshold [39].

It is hence of interest to determine whether data on the state is consistent with decays calculated in this work. Recently, the WA102 Collaboration reported evidence for two 2^{-+} states in central pp collisions at 450 GeV, which were absent in previous analyses by WA76 and WA91 at 85, 300 and 450 GeV [41]. The upper 2^{-+} state is found at 1840 $\pm$25 MeV with a width of 200$\pm$40 MeV. The observed decay mode is $a_2\pi$, in accordance with the predictions of this model and the IKP model. The Crystal Ball Collaboration reported some time ago a state with undecided J^{PC} (claimed to be 2^{-+}) at 1881$\pm$32$\pm$40 MeV, with a width of 221 $\pm$92$\pm$44 MeV, decaying equally to $a_2\pi$ and $a_0(980)\pi$ [47]. Similar conclusions were drawn by the CELLO Collaboration [47].

A doubling of isoscalar 2^{-+} peaks has also been reported by Crystal Barrel, in the isoscalar sector in $p\bar{p} \rightarrow (\eta\pi^o\pi^o)\pi^o$ [39]. Masses and widths of 1875$\pm$20 $\pm$35 MeV and 200$\pm$25$\pm$45 MeV have been reported for the upper 2^{-+} state. The high-mass state $\eta_2(1875)$ has been seen only in $f_2(1275)\eta$ (only 50 MeV above threshold), and no evidence of it is found in $a_0(980)\pi$, $f_0(980)\eta$, or $f_0(1370)\eta$. The absence of the state in $f_0(1370)\eta$ is consistent with the hybrid interpretation (see column 5 of Table III). However, the non-appearance of the state in $a_2\pi$ appears disasterous at first glance. We would like to point out

[4]Although LASS never claimed an isoscalar 2^{-+} resonance, the data appear to indicate an enhancement at 1.8–1.9 GeV in the 2^{-+} partial wave produced in $K^-p\rightarrow X\Lambda$, $X\rightarrow K_S^0K^\pm\pi^\mp$ (Fig. 2 of Ref. [42]). Since the production process may enhance $s\bar{s}$ above light quark production, LASS may have evidence for the $s\bar{s}$ nature of the enhancement.

TABLE IV. 2.0 GeV $s\bar{s}$ hybrid decay modes (MeV).

			alt	2.2 GeV hybrid	standard	IKP	reduced
2^{-+}	K^*K	P	6	13	11	8	82
	$K_2^*(1430)K$	S	28	29	21	44	
		D	.03	.5	.02	1	
	$K_1(1270)K$	D	.2	.5	.1	10	
	$K_0^*(1430)K$	D	.02	.3	.01	.2	
	$K_1(1400)K$	D	.06	.5	.03	.6	
	$f_2'(1525)\eta$	S	–	20	–	–	
		D	–	.2	–	–	
	$f_1(1510)\eta$	D	–	.03	–	–	
	$f_0(1370)\eta$	D	.01	.08	0	.1	
	$K^*(1410)K$	P	2	27	6	5	
	Γ (MeV)		36	91	38	69	
1^{-+}	$\eta'\eta$	P	0	0	0	0	44
	K^*K	P	6	13	11	8	82
	$K_2^*(1430)K$	D	.07	1	.04	∅	
	$K_1(1270)K$	S	14	10	11	14	
		D	3	8	2	21	
	$K_1(1400)K$	S	83	76	61	121	
		D	.03	.2	.02	.4	
	$f_2'(1525)\eta$	D	–	.04	–	–	
	$f_1(1510)\eta$	S	–	21	–	–	
		D	–	.02	–	–	
	$K(1460)K$	P	1	45	4	3	
	$\eta_s(1490)\eta$	P	–	15	–	–	
	$K^*(1410)K$	P	2	27	6	5	
	Γ (MeV)		109	216	95	172	
0^{-+}	K^*K	P	26	52	46	33	330
	$K_2^*(1430)K$	D	.4	6	.2	1	
	$K_0^*(1430)K$	S	113	117	83	174	
	$f_2'(1525)\eta$	D	–	.2	–	–	
	$f_0(1370)\eta$	S	72	105	64	109	
	$K^*(1410)K$	P	7	110	22	18	
	Γ (MeV)		218	390	215	335	
1^{--}	K^*K	P	13	26	23	16	165
	$\phi\eta$	P	2	19	11	3	89
	$\phi\eta'$	P	.01	2	.1	.02	.5
	$K_2^*(1430)K$	D	.1	2	.07	2	
	$K_1(1270)K$	S	23	16	18	24	
		D	.2	.6	.1	2	
	$K_1(1400)K$	S	43	40	32	63	
		D	.1	.6	.04	.7	
	$h_1(1380)\eta$	S			∅		
		D			∅		
		D	.07	.6	.04	.3	
	$K^*(1410)K$	P	3	55	11	9	
	Γ (MeV)		84	155	95	120	
2^{+-}	K^*K	D	1	3	2	1	13
	$\phi\eta$	D	.06	.8	.3	.08	2
	$\phi\eta'$	D	0	0	0	0	0
	$K_2^*(1430)K$	P	.3	1	.2	32	
		F	0	.03	0	.01	

TABLE IV. (*Continued*).

			alt	2.2 GeV hybrid	standard	IKP	reduced
	$K_1(1270)K$	P	.2	.3	.1	17	
		F	.04	.2	.02	.6	
	$K_1(1400)K$	P	3	8	2	28	
		F	0	0	0	0	
	$h_1(1380)\eta$	P	.3	2	.2	9	
		F	0	0	0	0	
	$K^*(1410)K$	D	.04	2	.1	.08	
	Γ (MeV)		5	18	5	79	
1^{+-}	K^*K	S	20	19	34	42	247
		D	.6	2	1	.6	7
	$\phi\eta$	S	11	63	66	28	523
		D	.03	.5	.2	.04	1
	$\phi\eta'$	S	2	19	8	3	61
		D	0	.02	0	0	0
	$K_2^*(1430)K$	P	8	35	5	10	
		F	0	.02	0	.01	
	$K_1(1270)K$	P	4	5	2	122	
	$K_0^*(1430)K$	P	3	14	2	18	
	$K_1(1400)K$	P	3	8	2	4	
	$h_1(1380)\eta$	P	$\varnothing$	$\varnothing$	$\varnothing$	14	
	$K^*(1410)K$	S	39	206	181	201	
		D	.02	1	.06	.04	
	Γ (MeV)		91	373	301	443	
0^{+-}	$K_1(1270)K$	P	66	95	43	165	
	$K_1(1400)K$	P	10	30	6	36	
	$h_1(1380)\eta$	P	8	42	5	4	
	$K(1460)K$	S	46	323	205	221	
	Γ (MeV)		130	490	259	426	
1^{++}	K^*K	S	10	9	17	21	123
		D	1	4	2	1	15
	$K_2^*(1430)K$	P	3	13	2	27	
		F	0	.05	0	.01	
	$K_1(1270)K$	P	7	11	5	37	
	$K_0^*(1430)K$	P	$\varnothing$	$\varnothing$	$\varnothing$	2	
	$K_1(1400)K$	P	6	16	3	29	
	$f_2'(1525)\eta$	P	–	2	–	–	
		F	–	0	–	–	
	$f_1(1510)\eta$	P	–	4	–	–	
	$f_0(1370)\eta$	P	$\varnothing$	$\varnothing$	$\varnothing$	2	
	$K^*(1410)K$	S	19	103	90	100	
		D	.05	2	.1	.08	
	Γ (MeV)		46	164	119	219	

here that this is in fact not the case. Experimentally,

$$\frac{\Gamma(\eta_2(1875)\to a_2^0\pi^0)BR(a_2^0\to\eta\pi^0)}{\Gamma(\eta_2(1875)\to f_2\eta)BR(f_2\to\pi^0\pi^0)} = 0(+0.8)[39] \text{ or } 0.7\pm0.4\ [40]. \quad (12)$$

Employing branching ratios from Ref. [15] and theoretical widths yields

$$\frac{\Gamma(\eta_2(1875)\to a_2\pi)\frac{0.145}{3}}{\Gamma(\eta_2(1875)\to f_2\eta)\frac{0.847}{3}} \gtrsim 1.1(+0.3) \quad (13)$$

in both this model and the IKP model for a 1.875 GeV hybrid. The mean value was obtained for the ''standard param-

TABLE V. 4.1 GeV $c\bar{c}$ hybrid decay modes (MeV).

			alt	4.4 GeV hybrid	standard	IKP	reduced
2^{-+}	D^*D	P	.5	.1	.8	4	19
	$D^{**}(2^+)D$	S	–	9	–	–	
		D	–	.2	–	–	
	$D^{**}(1_L^+)D$	D	–	.2	–	–	
	$D^{**}(0^+)D$	D	–	.2	–	–	
	$D^{**}(1_H^+)D$	D	–	.2	–	–	
	Γ (MeV)		.5	10	.8	4	
1^{-+}	D^*D	P	.5	.1	.8	4	19
	$D^{**}(2^+)D$	D	–	.5	–	–	
	$D^{**}(1_L^+)D$	S	–	1.2	–	–	
		D	–	2.5	–	–	
	$D^{**}(1_H^+)D$	S	–	25	–	–	
		D	–	0	–	–	
	Γ (MeV)		.5	29	.8	4	
0^{-+}	D^*D	P	2	.3	3	16	76
	$D^{**}(2^+)D$	D	–	2.5	–	–	
	$D^{**}(0^+)D$	S	–	25	–	–	
	Γ (MeV)		2	28	3	16	
1^{--}	D^*D	P	1	.2	1.5	8	38
	$D^{**}(2^+)D$	D	–	1	–	–	
	$D^{**}(1_L^+)D$	S	–	7	–	–	
		D	–	.3	–	–	
	$D^{**}(1_H^+)D$	S	–	10	–	–	
		D	–	.2	–	–	
	Γ (MeV)		1	19	1.5	8	
2^{+-}	D^*D	D	.2	.2	.3	1	7
	$D^{**}(2^+)D$	P	–	.5	–	–	
		F	–	.02	–	–	
	$D^{**}(1_L^+)D$	P	–	0	–	–	
		F	–	0	–	–	
	$D^{**}(1_H^+)D$	P	–	3	–	–	
		F	–	0	–	–	
	Γ (MeV)		.2	4	.3	1	
1^{+-}	D^*D	S	.3	.1	.5	8	12
		D	.1	.1	.1	.5	4
	$D^{**}(2^+)D$	P	–	13	–	–	
		F	–	.01	–	–	
	$D^{**}(1_L^+)D$	P	–	2	–	–	
	$D^{**}(0^+)D$	P	–	8	–	–	
	$D^{**}(1_H^+)D$	P	–	2.5	–	–	
	Γ (MeV)		.4	26	.6	8.5	
0^{+-}	$D^{**}(1_L^+)D$	P	–	25	–	–	
	$D^{**}(1_H^+)D$	P	–	15	–	–	
	Γ (MeV)		–	40	–	–	
1^{++}	D^*D	S	.2	.1	.3	1	6
		D	.2	.2	.3	.3	8
	$D^{**}(2^+)D$	P	–	5	–	–	
		F	–	.03	–	–	
	$D^{**}(1_L^+)D$	P	–	5	–	–	

TABLE V. (*Continued*).

		alt	4.4 GeV hybrid	standard	IKP	reduced
$D^{**}(0^+)D$	P	–	$\varnothing$	–	–	
$D^{**}(1_H^+)D$	P	–	5	–	–	
Γ (MeV)		.4	15	.6	1.3	

eters'' and the error corresponds to the ''alternative parameters.''[5] Equality is reached in the narrow resonance approximation. The ratio appears to be consistent with the large errors estimated from experiment.

We conclude that although $\eta_2(1875)$ can be $s\bar{s}\,^1D_2$; it is equally consistent with the hybrid interpretation. A critical discriminant between these possibilities would be the experimental confirmation of an isovector partner [13] since the hybrid candidate consists of light quarks.

B. Strangeonium hybrids

Strangeonium hybrids could be studied by intense photon beams at JLab, due to the strong affinity of the photon for $s\bar{s}$. Vector and 1^{+-} hybrids have non-negligible $\phi\eta$ couplings which could form a good search channel. Moreover, we note that some non-exotic hybrids are substantially narrower than their quarkonium partners, e.g. for $J^{PC}=1^{--}$ the hybrid has a width of $\sim$100 MeV in both models compared to the prediction for $^3D_1$ quarkonium of 650 MeV [13]. This generates the prospect of photoproduction of vector states beyond the well known $\phi(1680)$.

When the total widths of all $I=1$, $I=0$ and $s\bar{s}$ hybrids listed in Table IV are computed, we find that for ''standard parameters'' the average total widths of the three flavor varieties are very similar in both models (although $I=0$ are about $\sim$30% narrower). This dispels a popular misconception that $s\bar{s}$ hybrids should be narrower than light quark hybrids.

C. Charmonium hybrids

The widths of charmonium hybrids are suppressed below $D^{**}D$ threshold, where only D^*D and $D_s^*D_s$ modes are allowed, since these are the only open charm combinations where the wave functions of the two final states are different. Widths in Table V are in the 1–20 MeV range, and hence surprisingly narrow for charmonia at such high masses. However, when the hybrids are allowed to become more massive than the $D^{**}D$ threshold, the total widths increase drastically (see Fig. 2) to 4–40 MeV for 4.4 GeV hybrids (see column 5 in Table V). However, in this model (but not in the IKP model [48]) the 2^{+-} exotic remains narrow at 4 MeV. Finally, for the sake of completeness, we present bottomonium hybrid widths in Table VI. These tend to be very narrow and are not discussed here.

V. CONCLUSIONS

We have explored the implications of the hybrid decay model constructed in Ref. [6]. The model assumes the validity of the flux tube description of hybrids. The hybrid decay vertex is motivated by the heavy quark limit of the QCD Hamiltonian. It is essentially given by transverse gluon dissociation into a $q\bar{q}$ pair. Thus, the decay model is similar to earlier [3] hybrid decay models which assumed that constituent gluons produced $q\bar{q}$ pairs in the standard perturbative manner. The main difference is that the hybrid and the decay mechanism have been written in terms of the degrees of freedom appropriate to the flux tube model (i.e., phonons). In this sense, the model presented here is similar to ''$^3S_1$'' meson decay models whereas the IKP model is similar to $^3P_0$ models.

This similarity extends to amplitude ratios. Amplitude ratios serve as a sensitive probe of the decay vertex and may be used to test models. For example, S/D amplitude ratios tend to be significantly smaller in $^3P_0$ meson decay models than in $^3S_1$ models due to details of momentum routing. Because of this it has been shown that $^3P_0$ models are heavily favored by the data [18]. A similar situation exists between this model and that of IKP. For example, the S/D amplitude ratio for $2^{-+}(I=0)\to a_2\pi$ is roughly 2 in the IKP model while it is 250 in this model. Similarly the S/D ratio for $1^{-+}(I=1)\to b_1\pi$ is 5 in the IKP model and 40 in this model. One can envision a time when these ratios may be experimentally determined and the models distinguished.

Hybrid states that have small total widths should be accessible experimentally. We find that for ''standard parameters'' the total width of the $I=1$, $I=0$ and $s\bar{s}\,2^{-+}$ hybrids are less than 100 MeV in both models. Moreover, the same is true for $I=0\,1^{--}$ and $s\bar{s}\,2^{+-}$. The stability of these narrow widths in both models is significant, and necessitates experimental examination of these states. There are also states which are less than 100 MeV wide in this model, but not in the IKP model. These are the $I=1$ and $I=0\,2^{+-}$, the $I=0$ and $s\bar{s}\,1^{-+}$, the $I=0\,0^{--}$ and 0^{+-}. In general the IKP model and this one give similar decay widths (in large part because both obey the spin and S+P selection rules). However they differ dramatically in a few places. The most obvious is the anomalously narrow width of exotic 2^{+-} hybrids predicted by this model (less than 10 MeV). This surprising result needs to be accounted for in experimental searches and partial wave analyses. The channel $2^{+-}\to a_2\pi\to(\rho\pi)\pi\to 4\pi$ is especially important in this regard.

Other differences are in the total widths of the $0^{+-}(I=1)$ and $1^{+-}(I=0)$ hybrids, which we predict to be roughly 200 MeV, while IKP predict values 3 times larger. A larger discrepancy is in the $1^{++}(I=0)$ state which we predict to be 50 MeV wide, while IKP predict 450 MeV.

Among the conclusions of our survey of interesting hybrid candidates were the following. The $\rho(1450)$ remains enigmatic and further experimental study of this state is vital.

[5]For a light quark $^1D_2$ we find a ratio of 1.0 [13] and for a 2 $^1D_2$ a ratio of 0.7, all evaluated for a meson at 1.875 GeV.

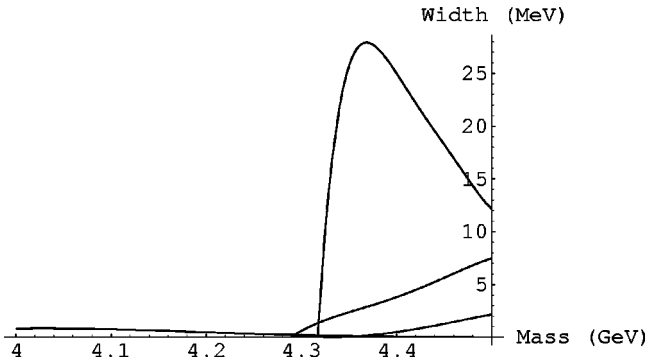

FIG. 2. Dominant partial widths of a $1^{-+}c\bar{c}$ hybrid at various masses. The partial widths to $D^{**}(1_H^+)D$, $D^{**}(1_L^+)D$, $D^{**}(2^+)D$ and D^*D correspond to the highest to the lowest intersections with the vertical axis.

This is especially true of the $a_1\pi$ mode which appears to be anomalously large.

Amongst quantum number-exotic hybrids, the isovector 0^{+-} appears to be very wide and thus may be difficult to detect. Alternatively, there is growing evidence for (several) 1^{-+} states. We stress the importance of exploring the $b_1\pi$ and $f_1\pi$ channels as well as $\pi\rho$ and, if the hybrid is heavy enough, $K_1(1400)K$. In fact the latter mode is expected to be the largest if the hybrid is heavier than 2.1 GeV.

The $\pi(1800)$ is difficult to accommodate as a conventional meson and makes a likely hybrid candidate. Indeed, the experimental branching ratios agree spectacularly with our predictions. Alternatively, it appears likely that the $a_1(1700)$ is a $2\,^3P_1$ quarkonium state due to the small S-wave $\pi\rho$ mode and the strong $f_1\pi$ channel. Finally, we conclude that the $\eta_2(1875)$ can be an $s\bar{s}\,^1D_2$ state or a hybrid. Searching for an isovector partner for this state would therefore be especially interesting.

All $c\bar{c}$ and $b\bar{b}$ hybrids are very narrow if they lie within their expected mass ranges. Since the heavy quarkonium spectrum is well understood, searches for these hybrids are especially interesting.

In general, all hybrid widths depend strongly on available phase space so that care should be exercised when employing our results. Furthermore, there can be substantial parameter dependence in the predicted widths. The standard and alternative data sets typically led to predictions differing by 50% and sometimes as much as 100%. Finally, the overall scale is not well known and may change substantially as new information emerges. We look forward to the day when hybrids and their decays are experimentally well established since this is doubtlessly an important step in developing an understanding of the mechanics of strong QCD and low energy glue.

ACKNOWLEDGMENTS

Financial support of the DOE under grants DE-FG02-96ER40944 (ESS) and DE-FG02-87ER40365 (A.P.S.) is acknowledged. P.R.P. acknowledges financial support from the English Speaking Union while he was at JLab, where part of this work was completed.

TABLE VI. 10.7 GeV $b\bar{b}$ hybrid decay modes (MeV).

				10.9 GeV			
			alt	hybrid	standard	IKP	reduced
2^{-+}	B^*B	P	.1	0	.5	3	44
1^{-+}	B^*B	P	.1	0	.5	3	44
0^{-+}	B^*B	P	.5	0	2	13	177
1^{--}	B^*B	P	.2	0	1.2	7	88
2^{+-}	B^*B	D	.08	.05	.25	1	22
1^{+-}	B^*B	S	.02	.1	.2	5	13
	B^*B	D	.02	.02	.15	.6	12
1^{++}	B^*B	S	.01	.05	.25	2	7
	B^*B	D	.1	.05	.5	1	24

APPENDIX

The ''standard parameters'' are as follows. All β's are those of Ref. [21], i.e., for $u\bar{u}$, $s\bar{s}$, $c\bar{c}$, $b\bar{b}$ hybrids 0.27, 0.30, 0.30, 0.34 GeV, for $a_2(1320)$, $a_1(1260)$, $a_0(1450)$, $b_1(1235)$, $f_2(1270)$, $f_1(1285)$, $f_0(1370)$, $h_1(1170)$, D^{**} 0.34 GeV, for $\pi(1300)$, $\rho(1450)$, $\omega(1420)$ 0.35 GeV, for $K(1460)$, $K_0^*(1410)$ 0.37 GeV, for $K_2^*(1430)$, $K_1(1270)$, $K_0^*(1430)$, $K_1(1400)$ 0.38 GeV, for π, ρ, ω, D, D^* 0.39 GeV, for B, B^*, $f_2'(1525)$, $f_1(1510)$, $f_0(1370)$, $h_1(1380)$ 0.41 GeV, for $\eta_u(1295)$ 0.42 GeV, for K, K^* 0.43 GeV, for $\eta_s(1490)$ 0.45 GeV, for $\phi(1680)$ 0.46 GeV, for η, η' 0.47 GeV and for ϕ 0.54 GeV. In the case of hybrid decays to S-wave mesons the widths are zero for $\beta_A=\beta_B$. The width divided by $(\beta_A^2-\beta_B^2)^2/(\beta_A^2+\beta_B^2)^2$ remains finite, and is called the ''reduced width.'' For hybrid decays to S-wave mesons we calculate the actual width by multiplying the reduced width by $(\beta_A^2-\beta_B^2)^2/(\beta_A^2+\beta_B^2)^2$, but this time we take the β's to be those of Ref. [12], i.e., for π 0.75 GeV, η,η' 0.74 GeV, ρ,ω 0.45 GeV, ϕ 0.51 GeV, K 0.71 GeV, K^* 0.48 GeV, D 0.66 GeV, D^* 0.54 GeV, B 0.64 GeV and B^* 0.57 GeV. We assume that the quarks that are created may have different mass than the initial quarks. Specifically, the mass of the u,s,c,b quarks are assumed to be 0.33, 0.55, 1.82, 5.12 GeV.

We assume $D_{0^{++}}^{**}$ and $D_{1^{+}H}^{**}$ (high mass 1^+ state) to have masses of 2.40 and 2.45 GeV respectively. The wave functions are taken to be S.H.O. wave functions except for the hybrid, where a radial prefactor of r^δ, with $\delta=0.62$ is assumed [21]. The $^3P_1/^1P_1$-mixing is 34° [38] in the P-wave kaon sector. $D_{1^+L}^{**}/D_{1^+H}^{**}$ mixing is 41°.

The ''alternative parameters'' (also employed in Ref. [6]) change from the preceding as follows. β of all hybrids are 0.3 GeV. β of $\pi,\rho,\omega,K,K^*,\phi,D,D^*,B,B^*$ are 0.54, 0.31, 0.31, 0.53, 0.36, 0.43, 0.45, 0.37, 0.43, 0.40 GeV respectively [49]. Other mesons have $\beta=0.35$ GeV [49]. We allow the final states to have different β's. All other conventions are the same as for the ''standard parameters.''

Note that the overall normalization of pair creation differs for ''standard'' and ''alternative'' parameters.

[1] UKQCD Collaboration, P. Lacock *et al.*, Phys. Lett. B **401**, 308 (1997); Phys. Rev. D **54**, 6997 (1996).

[2] D. Horn and J. Mandula, Phys. Rev. D **17**, 898 (1978).

[3] M. Tanimoto, Phys. Lett. **116B**, 198 (1982); A. Le Yaouanc, L. Oliver, O. Pene, J.-C. Raynal, and S. Ono, Z. Phys. C **28**, 309 (1985); F. Iddir, S. Safir, and O. Pene, Phys. Lett. B **433**, 125 (1998).

[4] N. Isgur and J. Paton, Phys. Rev. D **31**, 2910 (1985).

[5] N. Isgur, R. Kokoski, and J. Paton, Phys. Rev. Lett. **54**, 869 (1985).

[6] E. S. Swanson and A. P. Szczepaniak, Phys. Rev. D **56**, 5692 (1997).

[7] A. P. Szczepaniak and E. S. Swanson, Phys. Rev. D **55**, 3987 (1997).

[8] K. Juge, J. Kuti, and C. J. Morningstar, Nucl. Phys. B (Proc. Suppl.) **63**, 326 (1998).

[9] H. G. Dosch and D. Gromes, Phys. Rev. D **33**, 1378 (1986).

[10] P. R. Page, Phys. Lett. B **402**, 183 (1997).

[11] F. Iddir, A. Le Yaouanc, L. Oliver, O. Pene, and J. C. Raynal, Phys. Lett. B **207**, 325 (1988).

[12] R. Kokoski and N. Isgur, Phys. Rev. D **35**, 907 (1987).

[13] T. Barnes, F. E. Close, P. R. Page, and E. S. Swanson, Phys. Rev. D **55**, 4157 (1997).

[14] A. B. Clegg and A. Donnachie, Z. Phys. C **62**, 455 (1994).

[15] Particle Data Group, R. M. Barrett *et al.*, Phys. Rev. D **54**, 1 (1996).

[16] P. R. Page, Phys. Lett. B **401**, 313 (1997).

[17] P. R. Page, Nucl. Phys. **B495**, 268 (1997).

[18] P. Geiger and E. S. Swanson, Phys. Rev. D **50**, 6855 (1994).

[19] E. S. Swanson, Proceedings of the CMU/JLab Workshop on Physics with High Energy Photons, 1998 (Jefferson Lab).

[20] A. Le Yaouanc, L. Oliver, O. Pène, and J.-C. Raynal, Phys. Rev. D **29**, 1233 (1984); A. Le Yaouanc, L. Oliver, S. Ono, O. Pène, and J.-C. Raynal, *ibid.* **31**, 137 (1985); S. Adler and P. Davis, Nucl. Phys. **B244**, 469 (1984).

[21] F. E. Close and P. R. Page, Nucl. Phys. **B443**, 233 (1995); Phys. Rev. D **52**, 1706 (1995).

[22] F. E. Close and P. R. Page, Phys. Rev. D **56**, 1584 (1997).

[23] Crystal Barrel Collaboration, U. Thoma, in *Proceedings of Hadron '97*, Upton, NY, 1997, edited by S.-U. Chung and H. J. Willutzki, p. 332.

[24] 818 Collaboration, J. H. Lee *et al.*, Phys. Lett. B **323**, 227 (1994).

[25] VES Collaboration, A. M. Zaitsev, Proceedings of ICHEP'96 (Warsaw, 1996).

[26] E852 Collaboration, A. I. Ostrovidov *et al.* (unpublished).

[27] VES Collaboration, Yu. P. Gouz *et al.*, *Proceedings of the 26th International Conference on HEP* (Dallas, 1992), edited by J. R. Sanford (American Institute of Physics, New York, 1993), p. 572.

[28] CLAS Collaboration, S. Stepanyan *et al.*, ''Exotic Meson Spectroscopy with CLAS,'' CEBAF proposal PR 94-121.

[29] E852 Collaboration, D. R. Thompson *et al.*, Phys. Rev. Lett. **79**, 1630 (1997).

[30] CLAS Collaboration, W. Brooks *et al.*, ''Search for $J^{PC}=1^{-+}$ exotic meson,'' CEBAF proposal PR 94-118.

[31] A. M. Zaitsev (private communication).

[32] P. R. Page, in *Proceedings of PANIC'96* (Williamsburg, 1996), edited by C. Carlson (1996), p. 500, hep-ph/9607476.

[33] VES Collaboration, A. M. Zaitsev, Yad. Fiz. **59**, 1674 (1996).

[34] X.-Q. Li and P. R. Page, Eur. Phys. J. C **1**, 579 (1998).

[35] VES Collaboration, A. M. Zaitsev, *Proceedings of the 27th International Conference on High Energy Physics* (Glasgow, 1994), edited by P. Bussey and I. Knowles, p. 1409.

[36] VES Collaboration, D. Amelin *et al.*, Phys. Lett. B **356**, 595 (1995).

[37] VES Collaboration, D. Amelin, *Proceedings of Hadron '97* (Upton, NY, 1997) (Ref. [23]), p. 770.

[38] S. Godfrey and N. Isgur, Phys. Rev. D **32**, 189 (1985).

[39] CBAR Collaboration, C. Amsler *et al.*, Z. Phys. C **71**, 227 (1996).

[40] CBAR Collaboration, C. Amsler *et al.*, ''Study of $p\bar{p} \rightarrow \eta\pi^0\pi^0\pi^0$ at 1200 MeV/c.''

[41] WA102 Collaboration, D. Barberis *et al.*, hep-ex/9707021.

[42] D. Aston *et al.*, Phys. Lett. B **201**, 573 (1988).

[43] ARGUS Collaboration, H. Albrecht *et al.*, Z. Phys. C **74**, 469 (1997).

[44] L3 Collaboration, M. Acciarri *et al.*, CERN-PPE-97-068; EPS 1997 summer conference, Jerusalem (Abstract no. 474); S. Hou, *Proceedings of Hadron '97* (Upton, NY, 1997) (Ref. [23]), p. 745.

[45] T. Adams, Ph.D. thesis, Notre Dame University, 1997.

[46] UKQCD Collaboration, G. Bali *et al.*, Phys. Lett. B **309**, 378 (1993).

[47] Crystal Ball Collaboration, D. Antreasyan *et al.*, Z. Phys. C **48**, 561 (1990); Crystal Ball Collaboration, K. Karch *et al.*, *ibid.* **54**, 33 (1992); M. Feindt, *Proceedings of the 25th ICHEP* (Singapore, 1990), p. 537.

[48] P. R. Page, in *Proceedings of ''Quark Confinement and the Hadron Spectrum,''* edited by N. Brambilla and G. M. Prosperi (World Scientific, Singapore, 1994), p. 334, hep-ph/9410323.

[49] E. S. Swanson, Ann. Phys. (N.Y.) **220**, 73 (1992).